

Quantum Interference Due To Gravity and Precision Gravitational Red Shift

February 9, 2016

8.7 QUANTUM INTERFERENCE DUE TO GRAVITY

We now show how we can use path integrals to analyze a striking experiment illustrating the sensitivity of the neutron interferometer that we first introduced in Section 4.3. An essentially monochromatic beam of thermal neutrons is split by Bragg reflection by a perfect slab of silicon crystal at A. One of the beams follows path ABD and the other follows path ACD, as shown in Fig. 8.10. In general, there will be constructive or destructive interference at D depending on the path difference between these two paths. Suppose that the interferometer initially lies in a horizontal plane so that there are no gravitational effects. We then rotate the plane formed by the two paths by angle δ about the segment AC. The segment BD is now higher than the segment AC by $l_2 \sin \delta$. Thus there will be an additional gravitational potential energy $mg l_2 \sin \delta$ along this path, which alters the action and hence the amplitude to take the path BD by the factor

$$e^{-i(mg l_2 \sin \delta)T/\hbar} \quad (8.52)$$

where the action in the exponent is the negative of the potential energy multiplied by the time T it takes for the neutron to traverse the segment BD. Of course, gravity also affects the action in traversing the segment AB, but this phase shift

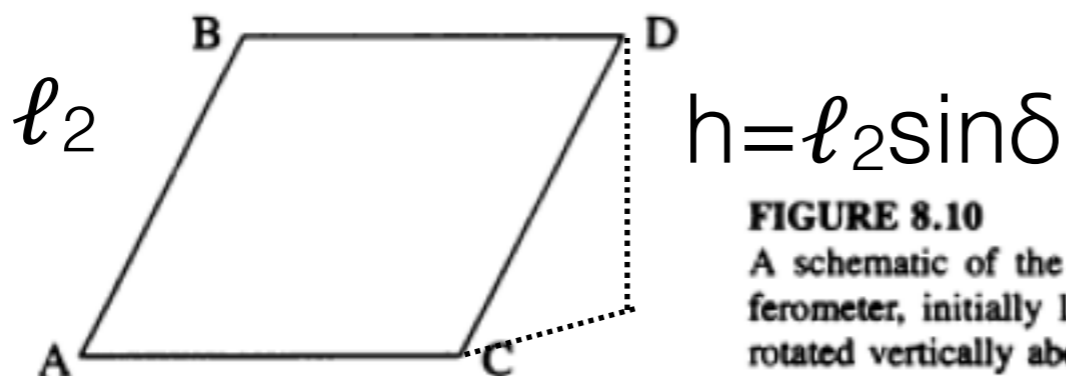


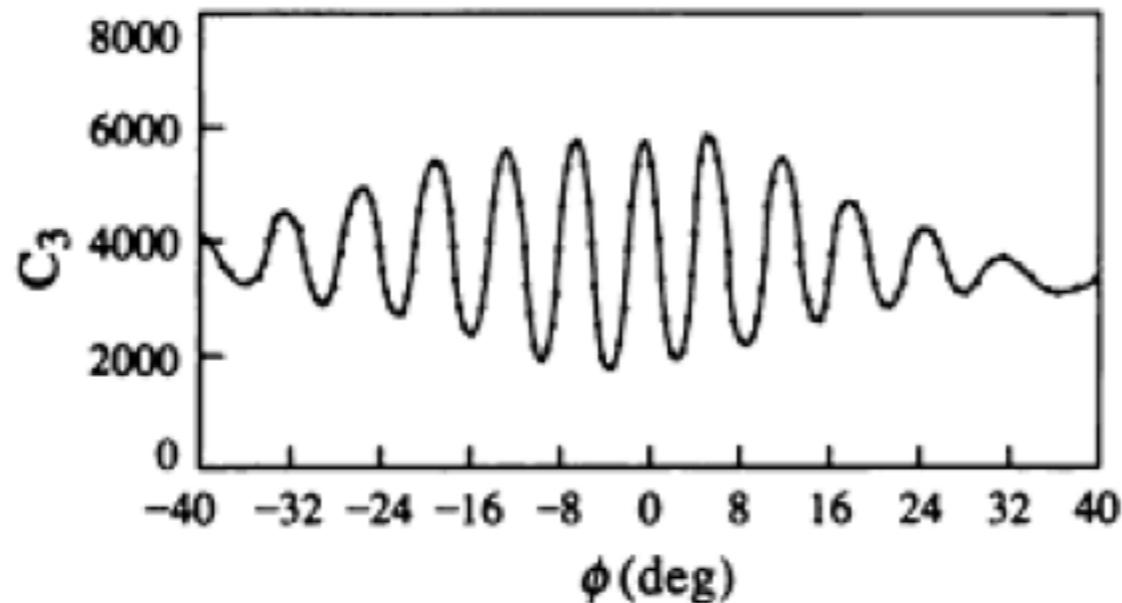
FIGURE 8.10

A schematic of the neutron interferometer. The interferometer, initially lying in a horizontal plane, can be rotated vertically about the axis AC by an angle δ .

is the same as for the segment CD, and thus the phase difference between the path ABD and the path ACD is given by

$$\begin{aligned} \frac{S[\text{ABD}] - S[\text{ACD}]}{\hbar} &= -\frac{mgl_2T \sin \delta}{\hbar} \\ &= -\frac{m^2gl_2l_1 \sin \delta}{\hbar p} \\ &= -\frac{m^2gl_2l_1 \lambda \sin \delta}{2\pi\hbar^2} \end{aligned} \quad (8.53)$$

where we have used the de Broglie relation $p = h/\lambda$ to express this phase difference in terms of the wavelength of the neutrons. Figure 8.11 shows the interference fringes that are produced as δ varies from -45° (BD below AC) to $+45^\circ$ (BD above AC) for neutrons with $\lambda = 1.419 \text{ \AA}$. The contrast of the interference pattern dies out with increasing angle of rotation because the interferometer bends and warps slightly (on the scale of angstroms) under its own weight as it is rotated about the axis AC.



1980, neutrons

FIGURE 8.11
The interference pattern as a function of the angle δ [From J.-L. Staudenmann, S. A. Werner, R. Colella, and A. W. Overhauser, *Phys. Rev. A* **21**, 1419 (1980).]

Measurement of gravitational acceleration by dropping atoms

Achim Peters, Keng Yeow Chung & Steven Chu

Physics Department, Stanford University, Stanford, California 94305-4060, USA

Here we use an atom interferometer based on a fountain of laser-cooled atoms to measure g , the acceleration of gravity. Through detailed investigation and elimination of systematic effects that may affect the accuracy of the measurement, we achieve an absolute uncertainty of $\Delta g/g = 3 \times 10^{-9}$, representing a million-fold increase in absolute accuracy compared with previous atom-interferometer experiments⁷. We also compare our measurement with the value of g obtained at the same laboratory site using a Michelson interferometer gravimeter (a modern equivalent of Galileo's 'leaning tower' experiment in Pisa). We show that the macroscopic glass object used in this instrument falls with the same acceleration, to within 7 parts in 10^9 , as a quantum-mechanical cesium atom.

$$\Delta g/g = 3 \times 10^{-9}$$

The absolute measurement in g of our atom interferometer was also compared to a falling corner cube instrument which has an estimated absolute accuracy of about two parts in 10^9

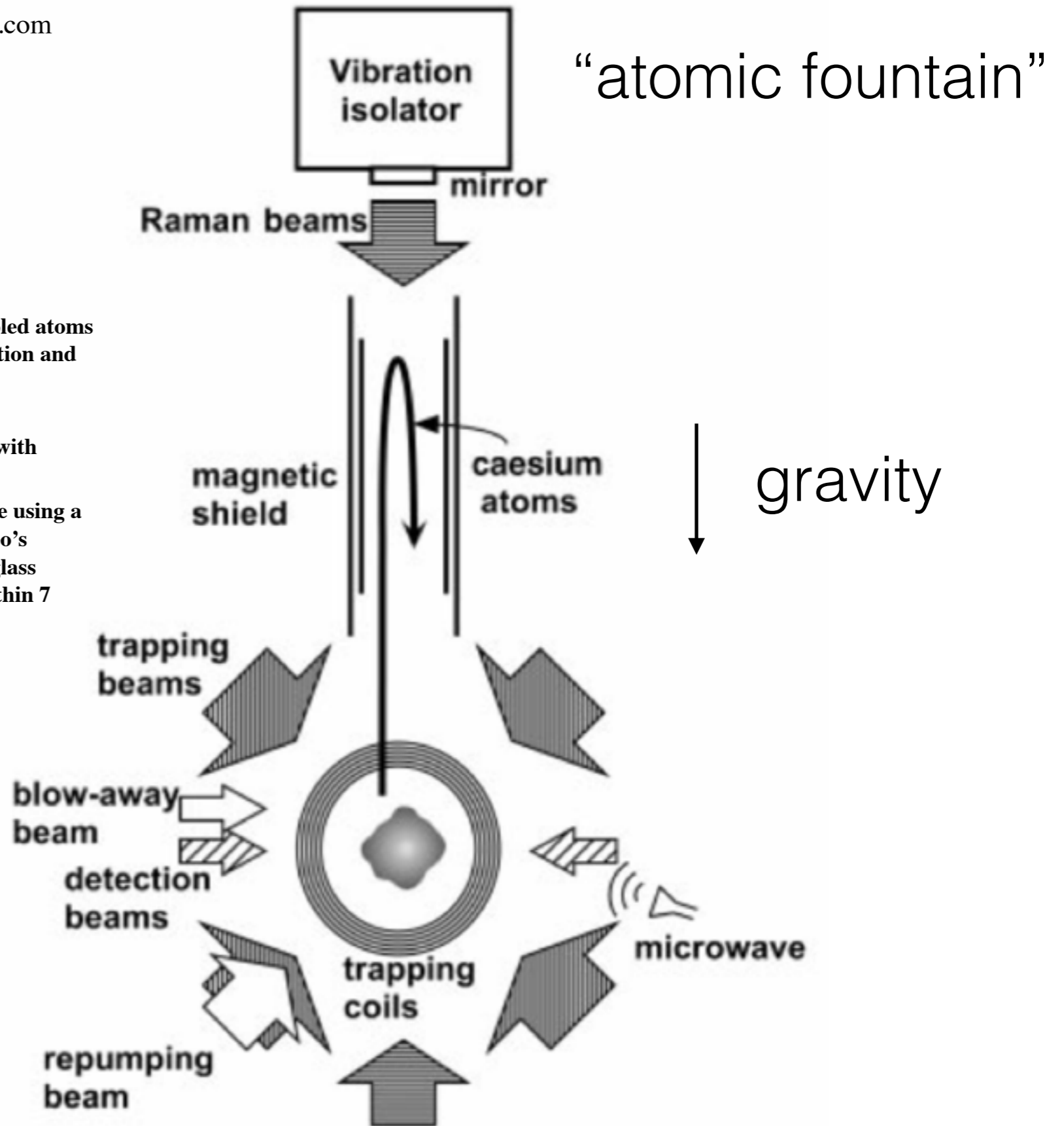


Figure 1 Overview of the experimental set-up.

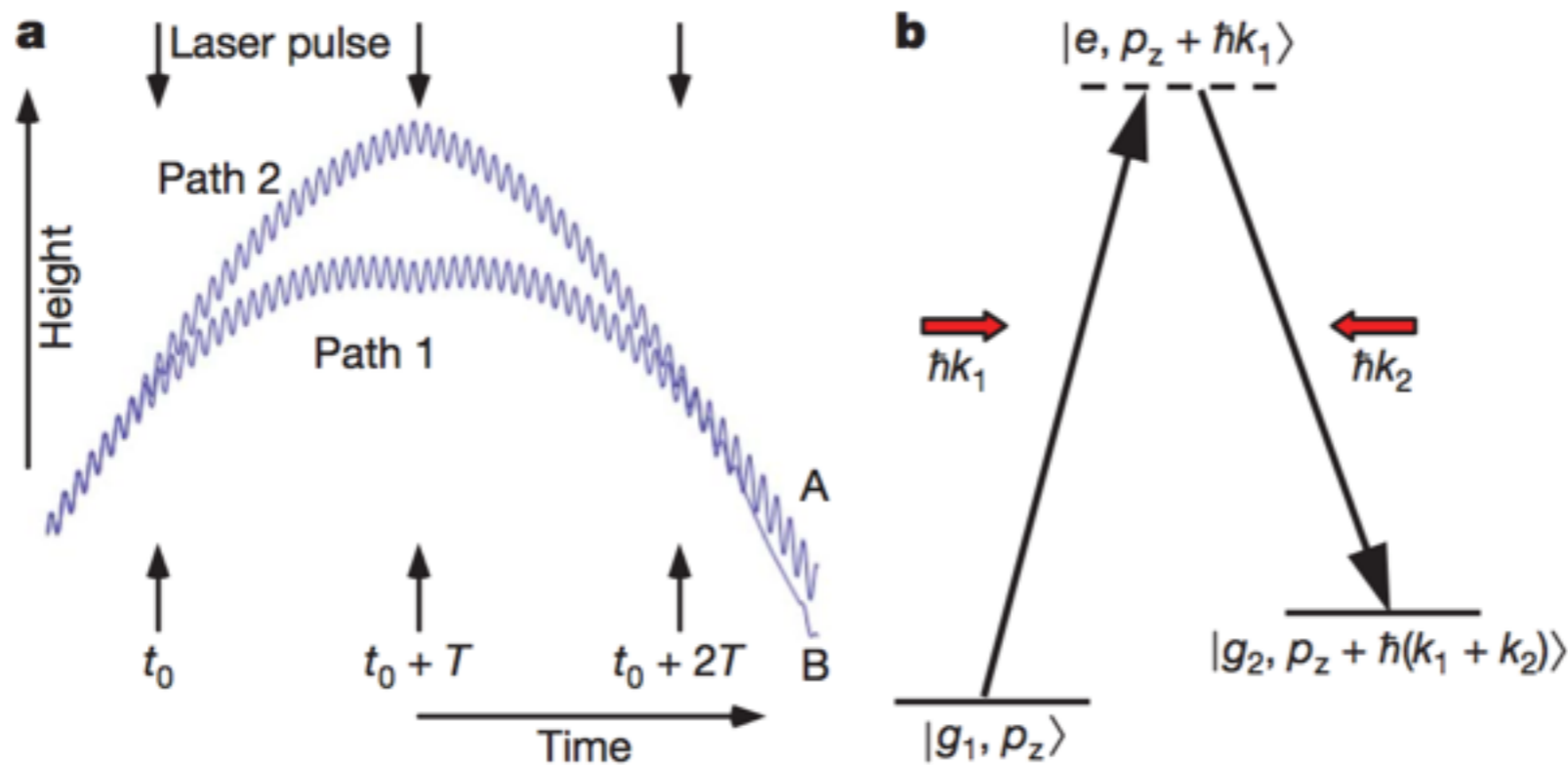


Figure 1 | Atom interferometer and Raman beam splitter. **a**, Atom interferometer (schematic). The trajectories of the atom are plotted as function of time in the laboratory frame of reference. They are accelerating owing to gravity. The oscillatory lines depict the phase accumulation of the matter waves. Arrows indicate laser pulses applied at times t_0 , $t_0 + T$ and $t_0 + 2T$ that change the trajectories. At time t_0 , the atom is put into a superposition of two trajectories. At time $t_0 + T$, a laser pulse is used to alter the trajectory of the atoms, and at time $t_0 + 2T$, the phase difference $\Delta\varphi = \Delta\varphi_2 - \Delta\varphi_1$ is recorded. **b**, Two-photon Raman beam splitter. An atom in a quantum state $|g_1, p_z\rangle$, moving upwards with momentum p_z , interacts with photons of two counter-propagating laser beams. The first one transfers the momentum $\hbar k_1$ and brings the atom into a virtual excited state $|e, p_z + \hbar k_1\rangle$. The second laser beam stimulates the atom to emit a photon of momentum $\hbar k_2$, which transfers the atom to another hyperfine ground state $|g_2, p_z + \hbar(k_1 + k_2)\rangle$. With appropriate duration and intensity of the laser pulses, the process can have 50% or 100% probability, creating beam splitters or mirrors for atomic matter waves.

2. Calculation of the interferometer phase shift ★

Consider a series of optical pulses used to construct an atom interferometer which measures the acceleration of gravity. The pulses cause the atom to enter a superposition of different internal states that spatially separate and recombine. From Feynman's formulation of quantum mechanics (Feynman & Hibbs 1965), the wave function $\Psi(z_b, t_b)$ at a spacetime point (z_b, t_b) is due to the contributions from all points (z_a, t_a) , (z'_a, t'_a) , $(z''_a, t''_a), \dots$ that end up at point (z_b, t_b) . For the contribution due to point (z_a, t_a) , the wave function is given by $\Psi(z_b, t_b) = e^{iS_{\text{Cl}}/\hbar} \Psi(z_a, t_a)$, where the classical action S_{Cl} is given by

$$S_{\text{Cl}} = \int_{t_a}^{t_b} L(z, \dot{z}) dt, \quad L(z, \dot{z}) = \frac{1}{2}M\dot{z}^2 - Mgz. \quad (2.1)$$

This expression is valid if the classical action S_{Cl} , defined by the integral over a path where the action is an extremum, is much greater than \hbar . Otherwise, we must sum the contributions to the action due to all allowed paths connecting (z_a, t_a) with (z_b, t_b) .

★Phil. Trans. R. Soc. Lond. A (1997) 355, 2223–2233

The action along the two paths (described on next page) is the same except for the absorption/emission of photons.

Adapted from

Phil. Trans. R. Soc. Lond. A

(1997) 355, 2223–2233

Three light pulses. Pulse 1 at $t = 0$ takes ground state $|1\rangle$ to excited state $|2\rangle$ by photon absorption with 50% probability. Pulse 2 at $t = T$ takes $|1\rangle \rightarrow |2\rangle$ by absorption $|2\rangle \rightarrow |1\rangle$ by stimulated emission with 100% probability. Pulse 3 takes at $t = 2T$ $|1\rangle \rightarrow |2\rangle$ by absorption $|2\rangle \rightarrow |1\rangle$ by stimulated emission with 50% probability. The experiment measures the fraction of atoms in state $|2\rangle$ at time $t = 2T$.

Amplitude for absorbing(-) or emitting(+) plane wave photon with probability 1/2:

$$A = \frac{1}{\sqrt{2}} \exp[\mp i(kz - \omega t - \phi)]$$

Trajectories, upper and lower. The atoms have an initial upward velocity v_0 . The absorption of a photon $p = \hbar k$ gives a change in velocity of V . The atomic states switch at time T .

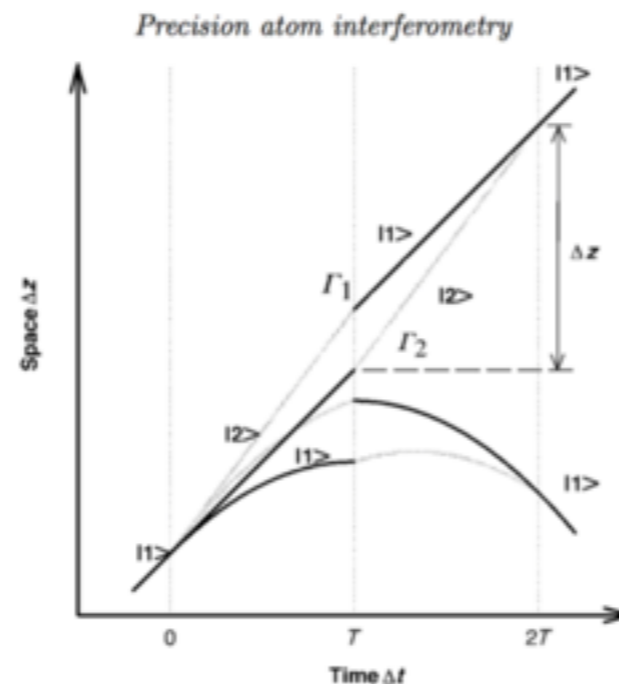


Figure 1: Upper (Γ_1) and lower (Γ_2) trajectories. $\Delta z = (v_0 + V)T$. From Phil. Trans. R. Soc. Lond. A (1997)

The upper trajectory is

$$z_u = \begin{cases} z_1 + (v_0 + V)t - \frac{1}{2}gt^2 & t < T \\ z_1 + (v_0 + V)T + (v_0 + V)(t - T) - \frac{1}{2}gt^2 & t > T \end{cases}$$

and the lower (down) trajectory

$$z_d = \begin{cases} z_1 + v_0t - \frac{1}{2}gt^2 & t < T \\ z_1 + v_0T + (v_0 + V)(t - T) - \frac{1}{2}gt^2 & t > T \end{cases}$$

The interference comes from the two paths. Path 1 – absorbs photon at $t = 0$, travels along z_u and emits photon at $t = T$, continues along z_d . Path 2– travels along z_d and absorbs photon at $t = T$, continues along z_u and emits photon at $t = 2T$. The total probability to measure the atom in state $|1\rangle$ at time $2T$ is

$$A^2 = |A_1 + A_2|^2$$

$$A_1 = \frac{1}{\sqrt{2}} \exp[-i(z_u(0) - \phi_1)] \exp[+i(kz_u(T) - \omega T - \phi_2)]$$

$$A_2 = \exp[-i(kz_d(T) - \omega T - \phi_2)] \frac{1}{\sqrt{2}} \exp[+i(kz_u(2T) - \omega 2T - \phi_3)]$$

Phase differences are

$$\begin{aligned} \Phi_1 &= k \left(z_1 + (v_0 + V)T - \frac{1}{2}gT^2 \right) - \omega T + (\phi_1 - \phi_2) = \\ & k(v_0 + V)T - k\frac{1}{2}gT^2 + (\phi_1 - \phi_2) \end{aligned}$$

and

$$\begin{aligned} \Phi_2 &= k \left(z_1 + (v_0 + V)T + v_0T - 2gT^2 - z_1 - v_0T + \frac{1}{2}gT^2 \right) - \omega T + (\phi_2 - \phi_3) = \\ & k(v_0 + V)T - k\frac{3}{2}gT^2 + (\phi_2 - \phi_3) \end{aligned}$$

Note that the term $k(v_0 + V)T$ ($\Delta z \equiv (v_0 + V)T$ in the figure) cancels between the two paths.

$$\Delta\Phi = \Phi_1 - \Phi_2 = kgT^2 + (\phi_1 - \phi_2) - (\phi_2 - \phi_3)$$

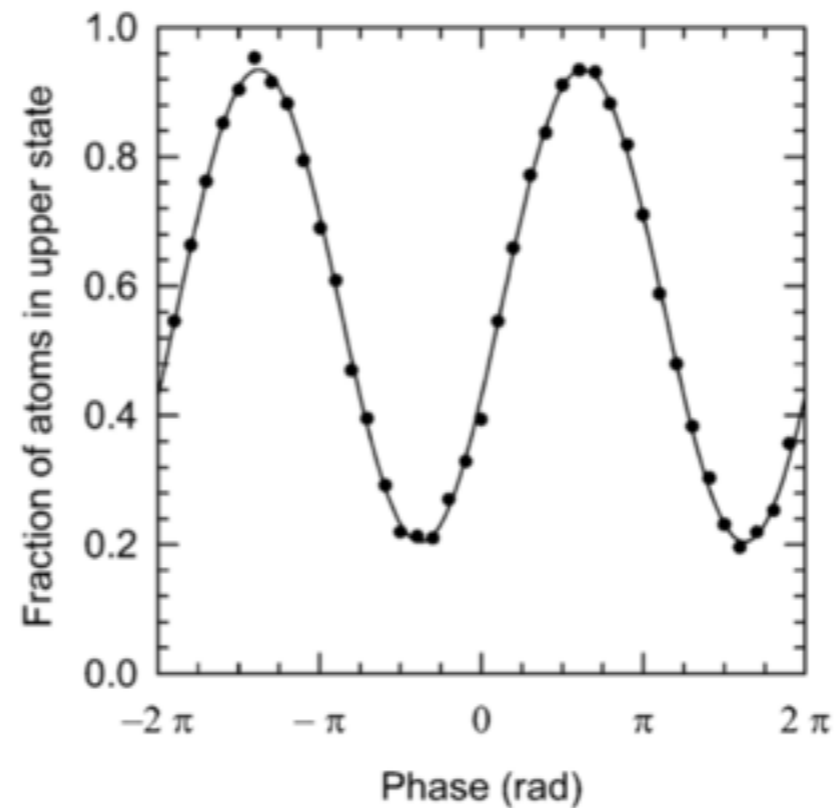


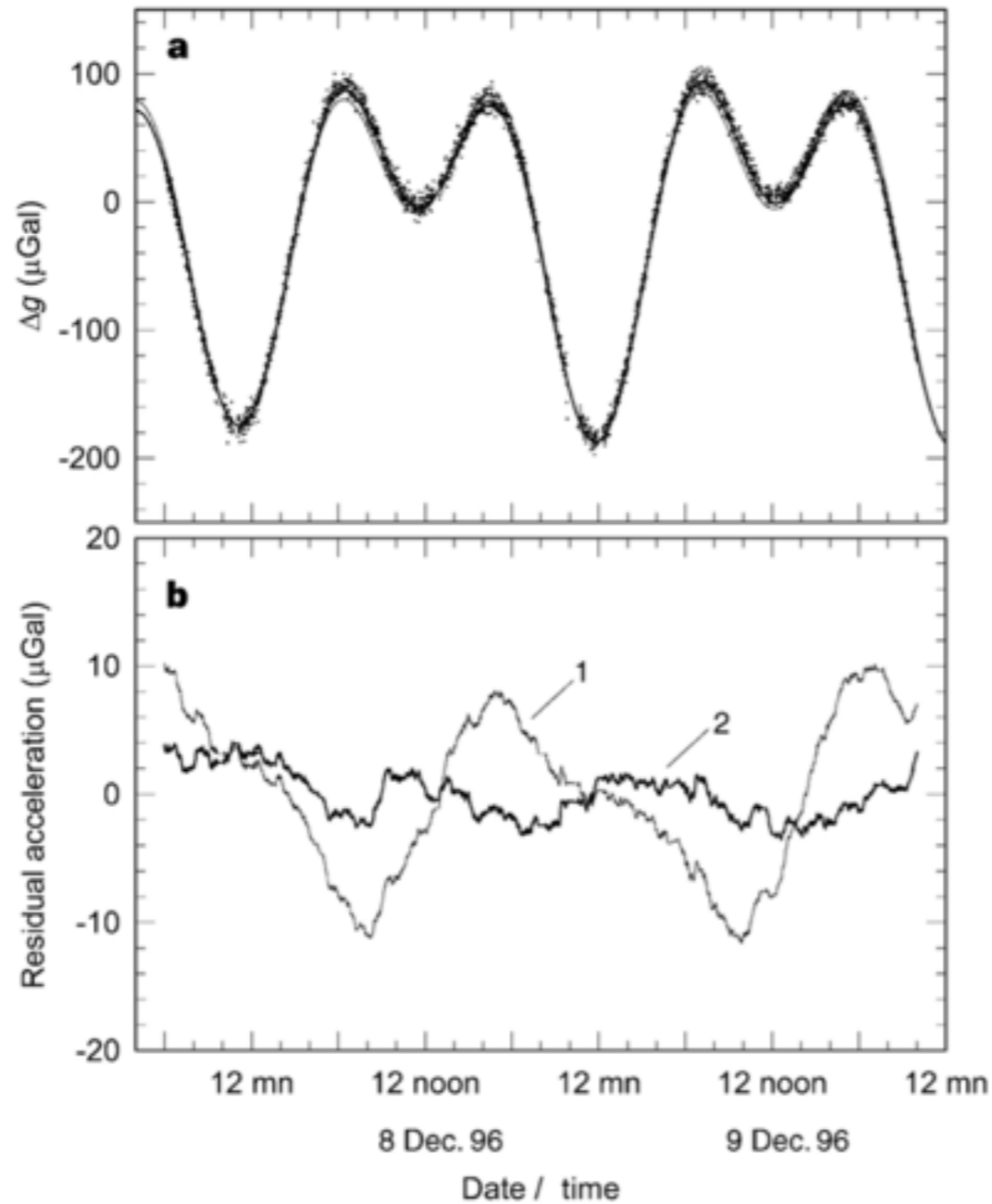
Figure 2 Typical Doppler-sensitive interferometer fringe for $T = 160$ ms. Shown are the 588,638th and 588,639th fringes. Each of the 40 data points represents a single launch of the atoms, spaced 1.3 s apart and taken over a period of 1 min. One full fringe corresponds to $\sim 2 \times 10^9 g$. Performing a least-squares fit determines local gravity to approximately $3 \times 10^{-9} g$.

$$\Delta\Phi = kgT^2 + (\phi_1 - \phi_2) - (\phi_2 - \phi_3)$$

Any slight difference in the frequency change between the frequency difference of the two optical beams and the falling atoms appears as a change in the population of the atoms in the excited state. In the actual experiment, we change the frequency in two discrete steps with a direct digital frequency synthesizer that changes its frequency in a phase continuous manner so that the relevant optical phase of the light is known. ★

$$P = \frac{1}{2} (1 + \cos \Delta\Phi)$$

★Phil. Trans. R. Soc. Lond. A (1997) 355, 2223–2233



data and
tidal models 1,2
2 includes oceans

residuals

Figure 3 Comparison between experimental data and tide models. **a**, A closer look at two days of gravity data. Each data point represents a one-minute gravity measurement. The solid lines represent two different tidal models. $1 \mu\text{Gal} = 10^{-8} \text{ m s}^{-2} \approx 10^{-9} g$. **b**, the residuals of the data with respect to a tidal model where (trace 1) the Earth is modelled as a solid elastic object and where (trace 2) the effects of ocean loading of the Earth are taken into account. Data for ocean loading were provided by H.-G. Scherneck. Effects at the few p.p.b. level, such as changes in the local barometric pressure, have not been included.

Table 2 The main known potential systematic effects

	Relative uncertainty (p.p.b.)
.....	
Systematic error	
Cs wavelength	0.3
Laser lock offset	0.4
r.f. phase shift	2
Coriolis effect	2
Gravity gradient	0.2
a.c. Stark shift	1
Dependence on pulse timing	1
.....	
Overall instrumental uncertainty	3.2
.....	
Environmental effect	
Pressure correction	1
Ocean loading	1
Other environmental effects	2

.....

Systematic effects that are ≤ 0.1 p.p.b. are not listed: these include possible effects of magnetic field gradients. The environmental effects are important in comparing values of g obtained at different times. Other environmental effects include water-table correction.

Extracting Gravitational Red Shift

$$\Delta\Phi_{red} = \frac{1}{\hbar} \int L(z, \dot{z}) d\tau =$$
$$-\frac{mc^2}{\hbar} \int \left[(1 + \beta) \frac{gz}{c^2} - \frac{\dot{z}^2}{2c^2} \right] dt$$

τ is proper time, first term is gravitational red shift, second term is time dilation, and β tests for anomalous gravity

The most accurate quantum mechanical gravity measurements to date have been performed with an interferometer using caesium atoms in an atomic fountain^{9,10}. After correcting for a number of relatively small fundamental^{10,17} and systematic¹⁰ effects (Table 1), the redshift is determined from the measured phase $\Delta\varphi$ as $z_{\text{meas}} = \Delta\varphi/(kT^2c^2)$. We find $z_{\text{meas}} = (1.090322683 \pm 0.0000000003) \times 10^{-16}$ per metre, where the standard error corresponds to a 3 parts per billion accuracy. The acceleration of gravity g varies with space and time owing to gravity gradients and tides. Thus, we used an absolute gravimeter (an FG-5 falling corner cube gravimeter) close by to measure g (corrected for systematic effects, such as elevation, air pressure, tides and polar motion¹⁰) and determine the locally expected redshift as $z_0 = g/c^2 = (1.090322675 \pm 0.0000000006) \times 10^{-16}$ per metre. These measurements refer to a particular location (1.810 m above the floor of the laboratory in Stanford, California). However, from the ratio of the measured and expected redshift, we obtain the redshift parameter $\beta = z_{\text{meas}}/z_0 - 1 = (7 \pm 7) \times 10^{-9}$, which is independent of local g and thus a universal constant of gravitation. It is compatible with general relativity within the standard error. This result has been achieved with a pulse separation time T of 160 ms and a peak separation of the trajectories of 0.12 mm. The experiment thus confirms local position invariance by excluding anomalous variations of more than 7 parts in 10^{28} of the frequency of the Compton clocks. This corresponds to comparing the elapsed times to $\sim 10^{-29}$ s.

measured

predicted

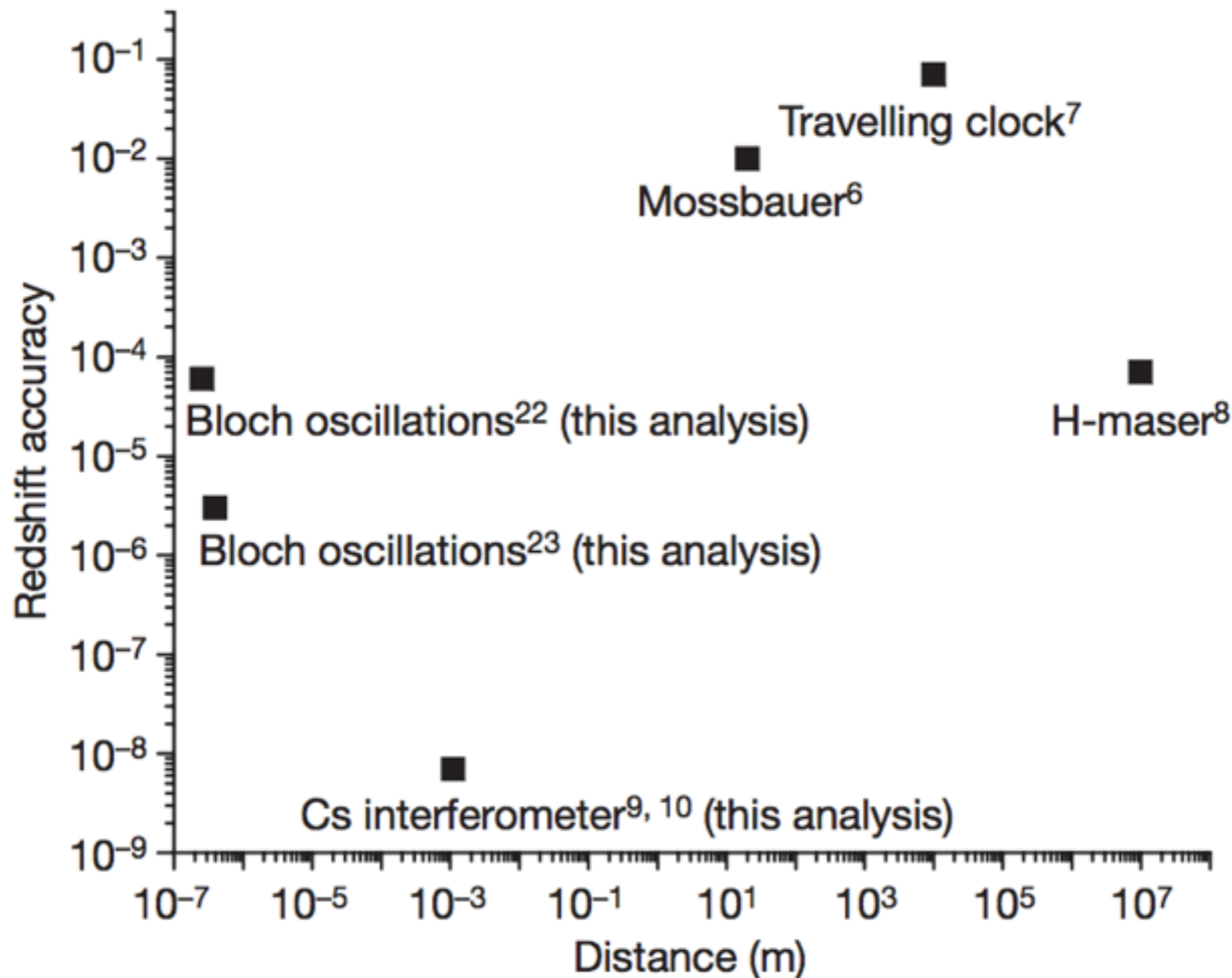


Figure 2 | Absolute determinations of the gravitational redshift. The accuracy (defined as the standard error) in β is plotted versus the relative height of the clocks.

6. Pound, R. V. & Snider, J. L. Effect of gravity on gamma radiation. *Phys. Rev.* **140**, B788–B803 (1965).